Acta Crystallographica Section B
Structural Science
ISSN 0108-7681

Isostructuralism among 'bridge-flipped' isomeric benzylideneanilines and phenylhydrazones

William H. Ojala,[a]* Jonathan M. Smieja,[a] Jill M. Spude,[a] Trina M. Arola,[a] Marika K. Kuspa,[a] Nell Herrera[a] and Charles R. Ojala[b]

[a]Department of Chemistry, University of St Thomas, St Paul, Minnesota 55105, USA, and [b]Department of Chemistry, Normandale Community College, Bloomington, Minnesota 55431, USA

Correspondence e-mail: whojala@stthomas.edu

Received 4 January 2007
Accepted 11 April 2007

'Bridge-flipped' isomers may be defined as pairs of molecules related by a reversal of a bridge of atoms connecting two major parts of the individual molecules. This kind of isomerism is commonly found among benzylideneanilines and phenylhydrazones. Isostructural pairs might be suitable for co-crystallization and are thus useful in the preparation of new solid materials. Although most of the examples of bridge-flipped isomeric benzylideneanilines and phenylhydrazones in the crystallographic literature are not isostructural, a small number of isostructural pairs have been reported by previous workers. This paper describes the molecular and crystal structures of four pairs of bridge-flipped isomers: two isostructural phenylhydrazones, (*E*)-2-bromobenzaldehyde 4-cyanophenylhydrazone (I) and (*E*)-4-cyanobenzaldehyde 2-bromophenylhydrazone (II); two pairs of isostructural benzylideneanilines, *N*-(2-trifluoromethylbenzylidene)-2-methylaniline (III) and *N*-(2-methylbenzylidene)-2-trifluoromethylaniline (IV), and *N*-(2-bromobenzylidene)-2-methylaniline (V) and *N*-(2-methylbenzylidene)-2-bromoaniline (VI); and a pair of benzylideneanilines with closely similar unit-cell dimensions but different packing arrangements, *N*-(4-methylbenzylidene)-4-cyanoaniline (VII) and *N*-(4-cyanobenzylidene)-4-methylaniline (VIII). The structure of (V) is disordered. The packing arrangement of (VIII) resembles that of the chloro-/methyl-substituted benzylideneanilines MBZCLA/MBZCLB [*N*-(4-methylbenzylidene)-4-chloroaniline and *N*-(4-chlorobenzylidene)-4-methylaniline]. Although intermolecular hydrogen bonding plays a part in the isostructuralism of the two phenylhydrazones, the other examples of isostructuralism occur in the absence of similar, relatively strong intermolecular interactions.

1. Introduction

Among the benzylideneaniline and phenylhydrazone families of organic compounds are found pairs of isomeric molecules related by a reversal of the orientation of the bridge of atoms

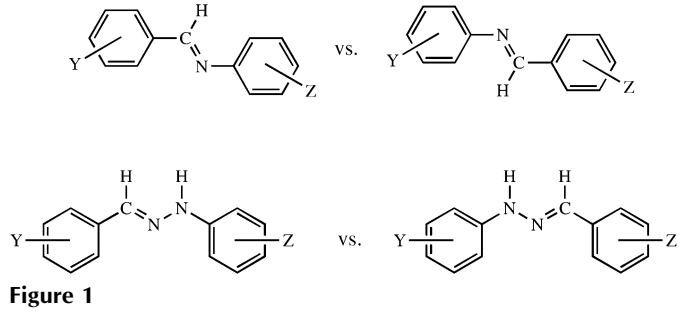

Figure 1
Bridge-flipped isomeric benzylideneanilines (upper) and phenylhydrazones (lower).

© 2007 International Union of Crystallography
Printed in Singapore – all rights reserved

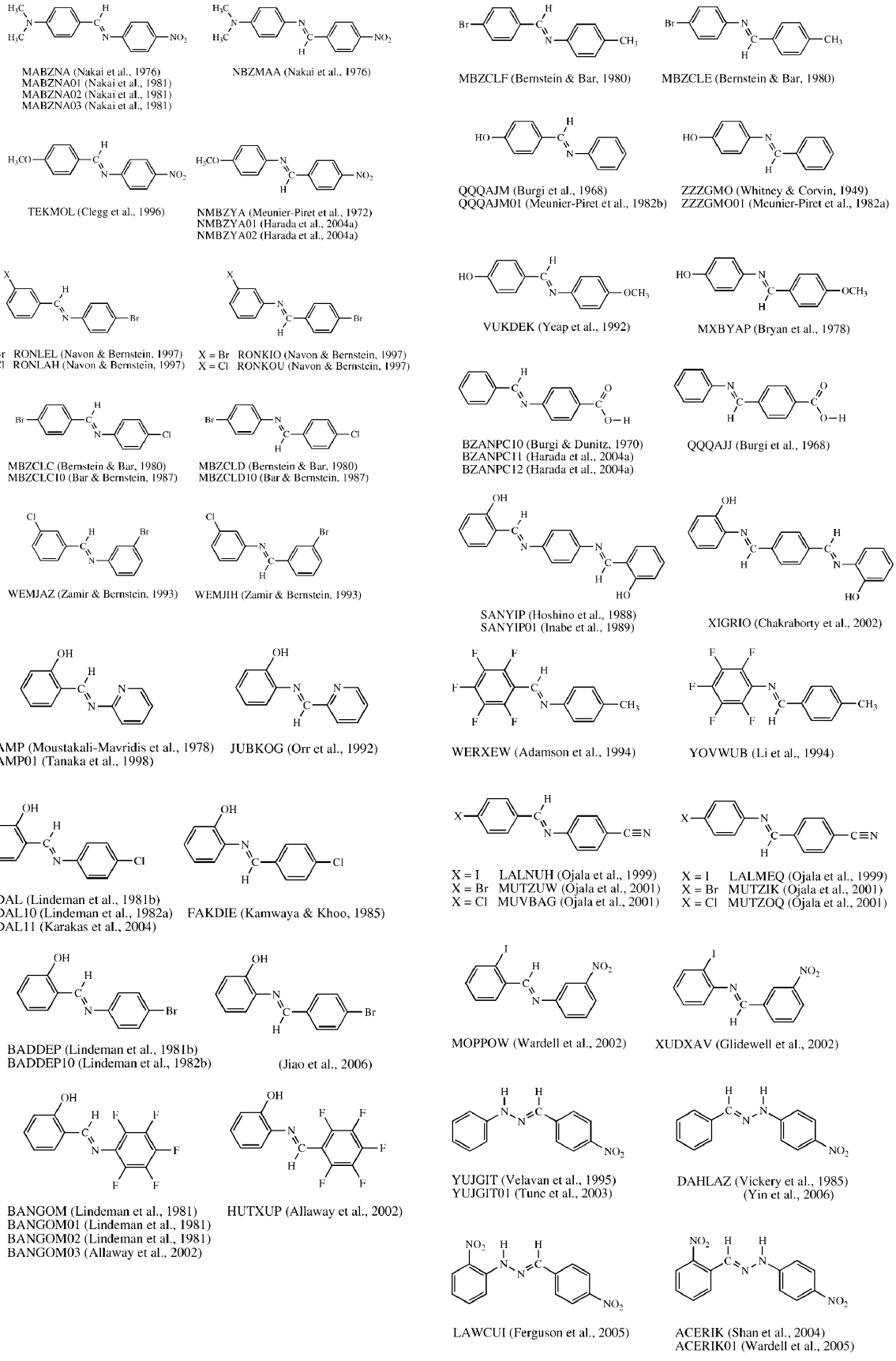

Figure 2
Non-isostructural 'bridge-flipped' benzylideneanilines and phenylhydrazones.

that links the aryl groups (Fig. 1). We have been examining the solid-state structures of these compounds to determine whether such pairs of 'bridge-flipped' isomers can assume similar packing arrangements. We are doing so with the goal of eventually using these isomers to prepare new solid materials. Pairs of bridge-flipped isomers, in particular those that form isostructural crystals, might be capable of co-crystallization from a suitable solvent, yielding materials with properties that can be systematically modified by co-crystallization of various proportions of the pure components. The color, melting point or conductivity of the new solid solution might be adjustable to any desired degree or extent for bridge-flipped isomers that are mutually soluble in the solid state. Recent work in both pharmaceutics (He *et al.*, 2001) and materials chemistry (Morimoto *et al.*, 2003) has demonstrated the usefulness of co-crystallization leading to solid-solution formation as a method of modifying solid-state properties such as transition temperature and photochromism. The exchange of the —CH═ group for —NH— or —N═ is a familiar strategy in drug development, in which these groups serve as bioisosteric replacements for each other (Silverman, 2004; Patani & LaVoie, 1996). The space-filling requirements of —CH═ and —N═ are sufficiently similar to allow isostructuralism and mixed-crystal formation between (for example) *trans*-stilbene and azobenzene (Bouwstra *et al.*, 1985).

On the other hand, whether a significant number of bridge-flipped isomeric pairs might be co-crystallized especially readily because they assume the same molecular packing arrangement in their respective crystals might appear doubtful in light of their record in the crystallographic literature. In Figs. 2 and 3 are listed the structures and refcodes of pairs of bridge-flipped isomeric benzylideneanilines and phenylhydrazones we have located in the Cambridge Structural Database (CSD Version 5.27 including updates through August 2006; Allen, 2002). Although our search has been done simply by surveying the CSD and not by means of a search algorithm that would ensure retrieval of every pair, we have made an effort to locate as many as do exist. Most of these pairs (those listed in Fig. 2) are not isostructural. Although the members of each pair have their own (potentially complex) set of reasons for assuming different packing arrangements, upon examining these structures it is possible to identify several common structural features that can differentiate the packing arrangements of bridge-flipped isomers from each other in general. Although the sheer number of non-isostructural pairs may seem discouraging for the prospects of isostructuralism and mutual solid-state solubility, an understanding of the features that differentiate these structures could be useful in efforts to design isostructural pairs.

A major structure-differentiating feature common particularly among benzylideneanilines is the difference in conformation that can exist between bridge-flipped isomers as a result of the difference in position of the bridge hydrogen atom. Steric interaction between this H atom and the aniline ring H atom *ortho* to the bridge can result in the twisting of the aniline ring further than the benzylidene ring out of coplanarity with the bridge atoms. The resulting difference in conformation between the two isomers contributes to their difference in crystal structure and is commonly found among the nonisostructural pairs listed in Fig. 2. Yet, at the same time, it is difficult to claim that this feature is the reason for the difference in packing arrangement between benzylideneaniline pairs in which one or both molecules are very nearly planar, as is true of NBZMAA, TEKMOL, RONKIO and RONKOU. In some cases the authors of these studies have identified other reasons for the structural differences, such as a preference for a particular type of intermolecular contact over another (*e.g.* N···halogen *versus* H···halogen interactions; Navon & Bernstein, 1997) that for reasons of molecular geometry or connectivity is accessible to only one of the two isomers.

Another differentiating feature is the change in position within the bridge of a hydrogen-bond donor or hydrogen-bond acceptor from one isomer to the other. In the case of the benzylideneanilines, the bridge N atom can serve as a hydrogen-bond acceptor in those derivatives that are substituted with hydrogen-bond donors on the rings. Changing the position of this acceptor within the bridge presumably contributes to the difference in crystal structure between QQQAJM/QQQAJM01 and ZZZGMO/ZZZGMO01, and also between VUKDEK and MXBYAP, as the hydroxyl group intermolecularly hydrogen bonds to the bridge N atom in all four structures. The role of hydrogen bonding in differentiating the structure in the BZANPC series from the structure QQQAJJ has yet to be determined, as only the cell

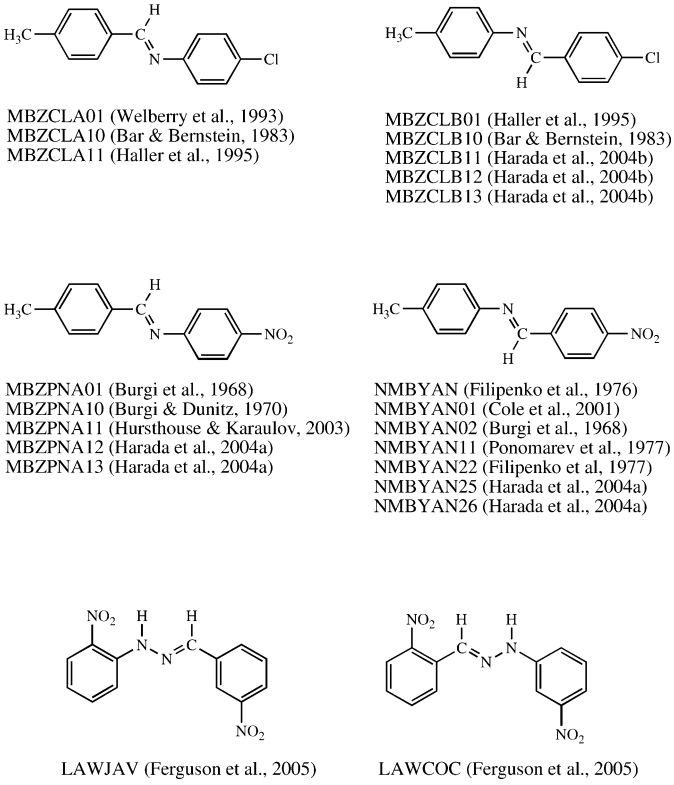

Figure 3
Isostructural benzylideneanilines and phenylhydrazones.

constants of QQQAJJ have been published thus far. The BZANPC series features the familiar centrosymmetric hydrogen-bonding interaction between carboxyl groups; the possible occurrence of this solid-state motif also in QQQAJJ should actually favor isostructuralism, in contrast to the previous examples. In the case of the phenylhydrazones, the bridging N—H group is a strong hydrogen-bond donor, and a difference in its bridge position in two isomers in which it participates in hydrogen bonding can cause differences in molecular packing between the two crystal structures. This effect is seen in the pair YUJGIT/YUJGIT01 and DAHLAZ, in which a two-pronged intermolecular contact involving the nitro group is shifted from its location in one isomer to a different location in the other (Fig. 4), a change in the intermolecular hydrogen-bonding motif that contributes to the difference in crystal structure between these isomers. In both structures the strongly hydrogen-bonding N—H group participates in the two-pronged hydrogen-bonding contact with the nitro group of a neighboring molecule as part of an $R_2^2(8)$ interaction, but in YUJGIT/YUJGIT01 this interaction is completed by a contact with the bridging C—H, whereas in DAHLAZ this contact is with a ring C—H *ortho* to the bridge, a C—H with enhanced hydrogen-bonding capability owing to the presence of the electron-withdrawing nitro group on the same ring. [That this change in the N—H position need not disrupt the solid-state hydrogen-bonding pattern in every case is demonstrated by the phenylhydrazones LAWJAV and LAWCOC (Ferguson *et al.*, 2005) in Fig. 3, and by the pair of isostructural phenylhydrazones we describe in this report.]

Hydrogen bonding as a structure-differentiating influence also occurs intramolecularly. A structural feature that contributes to differences in molecular packing between salicylideneanilines such as SANYIP/SANYIP01, SALAMP/SALAMP01, the BADDAL series, BADDEP/BADDEP10 and the BANGOM series on one hand and their *ortho*-aminophenol-based counterparts on the other is an intramolecular hydrogen bond to the bridge N atom that enforces a difference in molecular conformation (shown for the isomeric pair BANGOM02 and HUTXUP in Fig. 5) that can be expected to favor a difference in molecular-packing arrangement. The particular molecular conformation that allows this intramolecular hydrogen bond is found in every *ortho*-hydroxylated structure in Fig. 2. That this conformation is different for the two bridge-flipped isomers is a major obstacle to isostructuralism between the salicylideneanilines and the *N*-benzylidene-*o*-hydroxyanilines.

In spite of the variety of factors that discourage isostructuralism between bridge-flipped isomers, a few pairs have been found to be isostructural nonetheless. Fig. 3 shows the isostructural examples we have identified thus far in the crystallographic literature. A feature of particular significance in the 4-chloro-4-methyl benzylideneaniline pair MBZCLA/MBZCLB is their disorder, which involves an end-for-end flip of the molecule as well as a rotation of the molecule about the long molecular axis, resulting in the possibility of multiple orientations of the bridge. Disorder in the positions of benzylideneaniline bridge atoms is frequently observed (Bar & Bernstein, 1987; Zamir & Bernstein, 1993; Haller *et al.*, 1995; Ojala *et al.*, 2001; Harada *et al.*, 2004*a*,*b*), which suggests to us that if multiple orientations of the bridge can co-exist in a single crystal of a given benzylideneaniline, then it should be possible for crystals of bridge-flipped isomeric benzylideneanilines to differ in the orientation of the bridge and yet be structurally similar otherwise. (Disorder also exchanges the C—H and N—H positions within the bridge of isostructural phenylhydrazones; Ferguson *et al.*, 2005; Wardell *et al.*, 2005.) Co-crystallization of ordered, isostructural benzylideneanilines or phenylhydrazones would thus yield crystals disordered at the bridge atoms by design. Another isostructural pair is found among the polymorphs of the 4-methyl-4-nitro benzylideneanilines. The MBZPNA series includes three polymorphs, one orthorhombic and two monoclinic; the NMBYAN series includes two polymorphs, one triclinic and one monoclinic. The *Pc* polymorph of MBZPNA (structure MBZPNA11) is isostructural with the *Pc* polymorph of NMBYAN (structures NMBYAN01, NMBYAN02 and NMBYAN22). Neither the chloro–methyl isostructural pair nor the methyl–nitro isostructural pair shows any conformational differentiation owing to the interaction described above involving the aniline ring's *ortho* H atom and the bridging H atom; in both pairs the torsional angles defining the twist of the benzylidene and aniline rings out of the plane of the bridge atoms are similar. The molecules in MBZCLA/MBZCLB are located on crystallographic inversion centers and the molecules in the *Pc* polymorphs of MBZPNA/NMBYAN are nearly planar. In the pair of isostructural phenylhydrazones LAWJAV and LAWCOC, the structure-differentiating effect

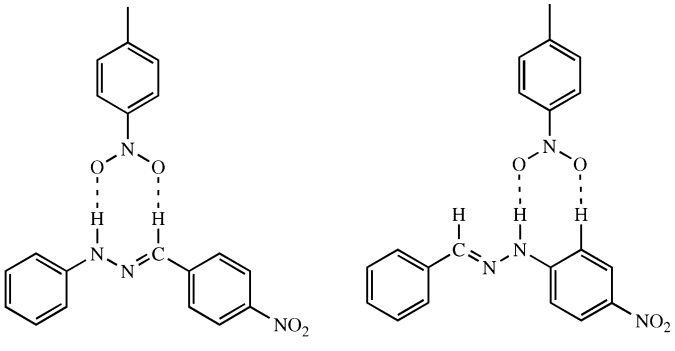

Figure 4
Intermolecular hydrogen-bonding interactions involving the nitro group in YUJGIT/YUJGIT01 (left) and DAHLAZ (right).

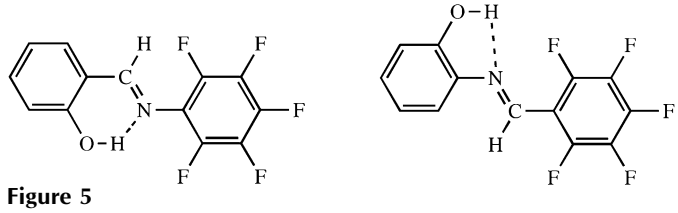

Figure 5
Conformations assumed by BANGOM02 (left) and HUTXUP (right) in the solid state. Both conformations facilitate intramolecular hydrogen bonding; at the same time they promote differences in molecular packing between the two structures.

Table 1
Experimental details, cell parameters and refinement results.

	(I)	(II)	(III)	(IV)	(V)
Crystal data					
Chemical formula	$C_{14}H_{10}BrN_3$	$C_{14}H_{10}BrN_3$	$C_{15}H_{12}F_3N$	$C_{15}H_{12}F_3N$	$C_{14}H_{12}BrN$
M_r	300.16	300.16	263.26	263.26	274.16
Cell setting, space group	Monoclinic, *Cc*	Monoclinic, *Cc*	Monoclinic, $P2_1/c$	Monoclinic, $P2_1/c$	Orthorhombic, *Pbcn*
Temperature (K)	173 (2)	173 (2)	173 (2)	173 (2)	173 (2)
a, *b*, *c* (Å)	4.2021 (3), 21.0409 (13), 14.3803 (9)	4.4902 (4), 19.9376 (17), 14.3182 (12)	9.6046 (6), 7.7953 (5), 17.2756 (11)	9.7556 (6), 7.8003 (5), 16.8794 (11)	13.4669 (10), 11.7471 (9), 14.9271 (11)
β (°)	96.248 (1)	92.884 (1)	104.316 (1)	102.647 (1)	90.00
V (Å^3)	1263.90 (14)	1280.20 (19)	1253.27 (14)	1253.30 (14)	2361.4 (3)
Z	4	4	4	4	8
D_x (Mg m^{-3})	1.577	1.557	1.395	1.395	1.542
Radiation type	Mo $K\alpha$	Mo $K\alpha$	Mo $K\alpha$	Mo $K\alpha$	Mo $K\alpha$
μ (mm^{-1})	3.24	3.20	0.11	0.11	3.45
Crystal form, colour	Needle, yellow	Needle, yellow	Prism, yellow	Prism, yellow	Prism, yellow
Crystal size (mm)	0.50 × 0.20 × 0.20	0.50 × 0.15 × 0.15	0.50 × 0.50 × 0.18	0.50 × 0.35 × 0.10	0.50 × 0.50 × 0.08
Data collection					
Diffractometer	Bruker SMART Platform CCD	Siemens SMART Platform CCD	Siemens SMART Platform CCD	Siemens SMART Platform CCD	Siemens SMART Platform CCD
Data collection method	Area detector, ω scans per φ	Area detector, ω scans per φ	Area detector, ω scans per φ	Area detector, ω scans per φ	Area detector, ω scans per φ
Absorption correction	Multi-scan (based on symmetry-related measurements)	Multi-scan (based on symmetry-related measurements)	Multi-scan (based on symmetry-related measurements)	Multi-scan (based on symmetry-related measurements)	Multi-scan (based on symmetry-related measurements)
T_{min}	0.462	0.565	0.942	0.951	0.194
T_{max}	0.521	0.616	0.977	0.986	0.756
No. of measured, independent and observed reflections	6085, 2202, 2082	6162, 2226, 2132	11 890, 2226, 2044	10 706, 2205, 1947	21 446, 2088, 1788
Criterion for observed reflections	$I > 2\sigma(I)$	$I > 2\sigma(I)$	$I > 2\sigma(I)$	$I > 2\sigma(I)$	$I > 2\sigma(I)$
R_{int}	0.023	0.024	0.018	0.018	0.034
θ_{max} (°)	25.0	25.0	25.1	25.1	25.1
Refinement					
Refinement on	F^2	F^2	F^2	F^2	F^2
$R[F^2 > 2\sigma(F^2)]$, $wR(F^2)$, S	0.026, 0.061, 1.04	0.024, 0.053, 1.06	0.032, 0.084, 1.05	0.028, 0.075, 1.04	0.027, 0.063, 1.10
No. of reflections	2202	2226	2226	2205	2088
No. of parameters	167	167	173	173	196
H-atom treatment	Mixture of independent and constrained refinement	Mixture of independent and constrained refinement	Constrained to parent site	Constrained to parent site	Constrained to parent site
Weighting scheme	$w = 1/[\sigma^2(F_o^2) + (0.0102P)^2 + 1.0482P]$, where $P = (F_o^2 + 2F_c^2)/3$	$w = 1/[\sigma^2(F_o^2) + (0.0003P)^2 + 0.4653P]$, where $P = (F_o^2 + 2F_c^2)/3$	$w = 1/[\sigma^2(F_o^2) + (0.0424P)^2 + 0.3704P]$, where $P = (F_o^2 + 2F_c^2)/3$	$w = 1/[\sigma^2(F_o^2) + (0.0344P)^2 + 0.3477P]$, where $P = (F_o^2 + 2F_c^2)/3$	$w = 1/[\sigma^2(F_o^2) + (0.0232P)^2 + 1.5024P]$, where $P = (F_o^2 + 2F_c^2)/3$
$(\Delta/\sigma)_{max}$	0.001	0.002	< 0.0001	< 0.0001	0.001
$\Delta\rho_{max}$, $\Delta\rho_{min}$ (e Å^{-3})	0.55, −0.52	0.29, −0.34	0.16, −0.24	0.17, −0.20	0.26, −0.22
Absolute structure	Flack (1983), 1087 Friedel pairs	Flack (1983), 1085 Friedel pairs	–	–	–
Flack parameter	0.036 (10)	0.030 (9)	–	–	–

	(VI)	(VII)	(VIII)
Crystal data			
Chemical formula	$C_{14}H_{12}BrN$	$C_{15}H_{12}N_2$	$C_{15}H_{12}N_2$
M_r	274.16	220.27	220.27
Cell setting, space group	Orthorhombic, *Pbcn*	Monoclinic, $P2_1/n$	Monoclinic, $P2_1/n$
Temperature (K)	173 (2)	173 (2)	173 (2)
a, *b*, *c* (Å)	13.3550 (12), 11.6667 (11), 14.9529 (14)	6.1535 (9), 7.1990 (10), 26.253 (4)	6.1878 (12), 7.3785 (15), 25.895 (5)
β (°)	90.00	92.285 (2)	94.635 (3)
V (Å^3)	2329.8 (4)	1162.1 (3)	1178.4 (4)
Z	8	4	4
D_x (Mg m^{-3})	1.563	1.259	1.242
Radiation type	Mo $K\alpha$	Mo $K\alpha$	Mo $K\alpha$
μ (mm^{-1})	3.50	0.08	0.07
Crystal form, colour	Prism, yellow	Plate, yellow	Prism, yellow
Crystal size (mm)	0.45 × 0.30 × 0.15	0.50 × 0.48 × 0.05	0.43 × 0.30 × 0.30

Table 1 (continued)

	(VI)	(VII)	(VIII)
Data collection			
Diffractometer	Siemens SMART Platform CCD	Siemens SMART Platform CCD	Siemens SMART Platform CCD
Data collection method	Area detector, ω scans per φ	Area detector, ω scans per φ	Area detector, ω scans per φ
Absorption correction	Multi-scan (based on symmetry-related measurements)	Multi-scan (based on symmetry-related measurements)	Multi-scan (based on symmetry-related measurements)
T_{min}	0.293	0.960	0.971
T_{max}	0.589	0.993	0.975
No. of measured, independent and observed reflections	21 202, 2059, 1865	10 066, 2062, 1727	2677, 2677, 2218
Criterion for observed reflections	$I > 2\sigma(I)$	$I > 2\sigma(I)$	$I > 2\sigma(I)$
R_{int}	0.031	0.023	–
θ_{max} (°)	25.0	25.0	27.6
Refinement			
Refinement on	F^2	F^2	F^2
$R[F^2 > 2\sigma(F^2)]$, $wR(F^2)$, S	0.029, 0.067, 1.13	0.037, 0.093, 1.06	0.065, 0.186, 1.07
No. of reflections	2059	2062	2677
No. of parameters	146	155	155
H-atom treatment	Constrained to parent site	Constrained to parent site	Constrained to parent site
Weighting scheme	$w = 1/[\sigma^2(F_o^2) + (0.0269P)^2 + 2.7709P]$, where $P = (F_o^2 + 2F_c^2)/3$	$w = 1/[\sigma^2(F_o^2) + (0.0412P)^2 + 0.2659P]$, where $P = (F_o^2 + 2F_c^2)/3$	$w = 1/[\sigma^2(F_o^2) + (0.091P)^2 + 0.6802P]$, where $P = (F_o^2 + 2F_c^2)/3$
$(\Delta/\sigma)_{max}$	0.001	<0.0001	0.013
$\Delta\rho_{max}$, $\Delta\rho_{min}$ (e Å^{-3})	0.38, −0.35	0.11, −0.14	0.31, −0.26

Computer programs used: *SMART* (Bruker, 2001), *SAINT* (Bruker, 2003), *SHELXS*97 (Sheldrick, 1990), *SHELXL*97 (Sheldrick, 1997), *PLATON* (Spek, 2003).

of moving the strongly hydrogen-bonding N—H group to a different position in the bridge is mitigated by a multi-point intermolecular hydrogen-bonding interaction in which the bridge N—H and the bridge C—H are both in contact with the same O atom from the nitro group of a neighboring molecule. Exchanging the positions of the C—H and N—H moieties does not disrupt this $R_2^1(6)$ hydrogen-bonding motif. In an additional, intramolecular interaction, the N—H group in

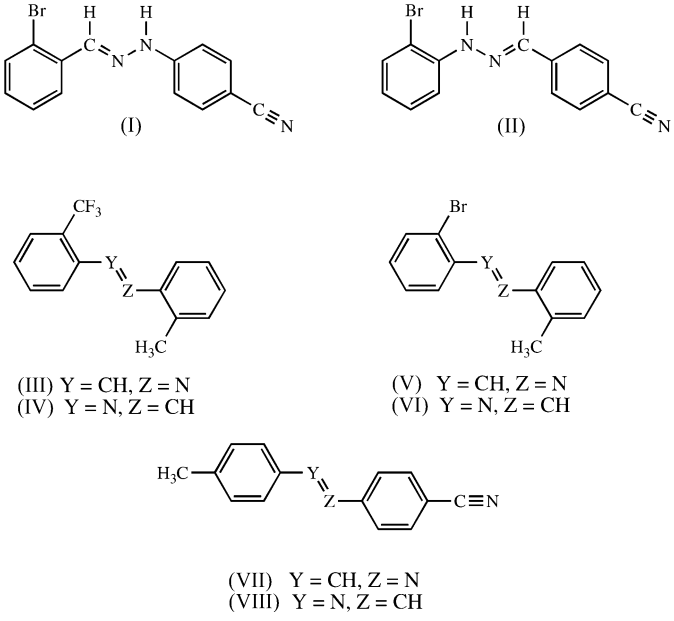

Figure 6
Bridge-flipped isomeric phenylhydrazones and benzylideneanilines described in this paper.

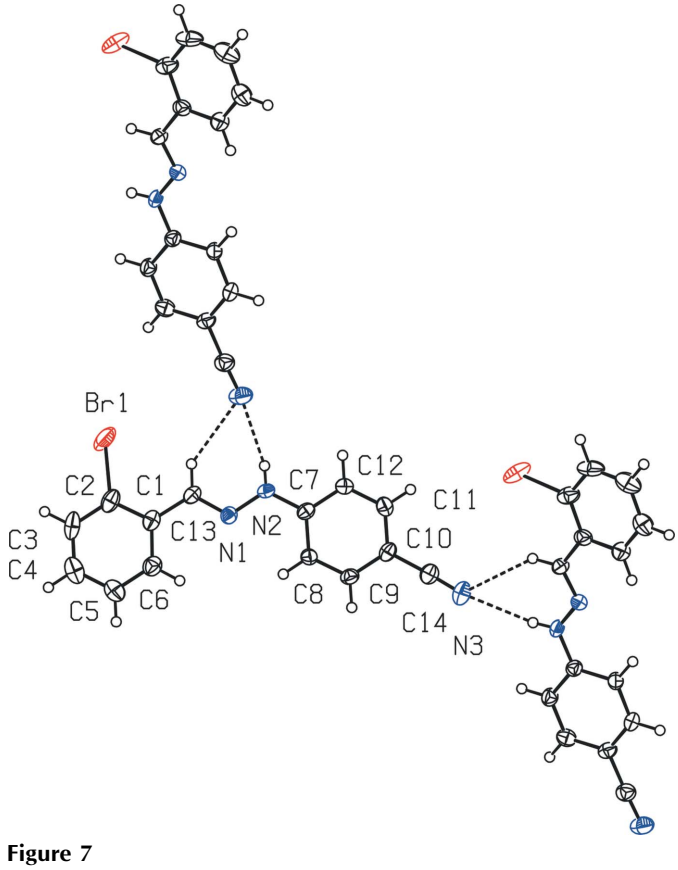

Figure 7
Close intermolecular contacts involving the cyano group in the packing arrangement of (I). Anisotropic displacement ellipsoids are shown at the 50% probability level. For clarity, the outline of the unit cell has been omitted. Symmetry-equivalent molecules shown in addition to the *xyz* molecule (labeled) are $\frac{3}{2}+x, \frac{3}{2}-y, \frac{1}{2}+z$ (top) and $-\frac{3}{2}+x, \frac{3}{2}-y, -\frac{1}{2}+z$ (right).

Table 2
Angles (°) between least-squares planes in (I) and (II).

	$A \angle B$	$C \angle B$
(I)	9.70 (0.32)	5.71 (0.34)
(II)	4.82 (0.33)	6.37 (0.32)

A = plane defined by ring atoms C1–C6; B = plane defined by bridge atoms N1, N2 and C13; C = plane defined by ring atoms C7–C12.

LAWJAV and the C—H group in LAWCOC are in close contact with the nitro group located *ortho* to them by virtue of their proximity to it; the C—H group assumes the same structural role as the N—H group, and the exchange of one group for the other causes no disruption to the packing arrangement common to LAWJAV and LAWCOC.

In attempting to make our own pursuit of isostructural bridge-flipped isomers systematic, we have been guided in part by results we obtained in our analysis of the non-isostructural pair of iodo-/cyano-substituted benzylideneanilines LALNUH and LALMEQ (Ojala *et al.*, 1999). In both structures a close contact of the Lewis acid–Lewis base type exists in the solid state between the I atom of a given molecule and the nitrile N atom of an adjacent molecule. This contact links molecules in the two crystal structures into similar chains. The structures

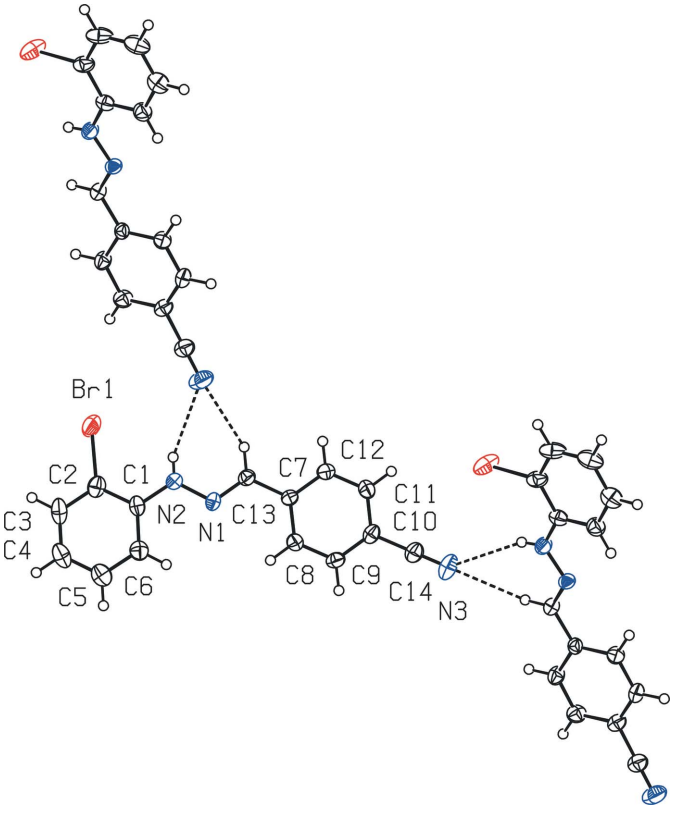

Figure 8
Close intermolecular contacts involving the cyano group in the packing arrangement of (II). Anisotropic displacement ellipsoids are shown at the 50% probability level. For clarity, the outline of the unit cell has been omitted. Symmetry-equivalent molecules shown in addition to the *xyz* molecule (labeled) are $\frac{3}{2}+x, \frac{3}{2}-y, \frac{1}{2}+z$ (top) and $-\frac{3}{2}+x, \frac{3}{2}-y, -\frac{1}{2}+z$ (right).

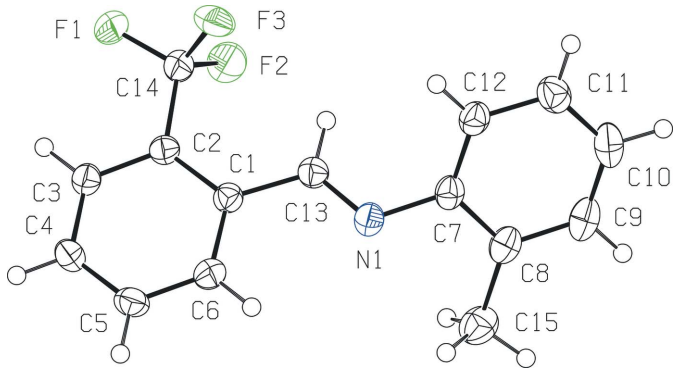

Figure 9
Molecular structure of (III), showing the atom numbering. Anisotropic displacement ellipsoids are shown at the 50% probability level.

differ in how layers of these molecular chains are stacked; nonetheless, the fact that the Lewis acid–Lewis base contact helps enforce packing similarity on at least one level of structure has encouraged us to examine additional halogen-nitrile compounds among both the benzylideneanilines and the phenylhydrazones. Here we describe the molecular packing arrangement we have found to be common to (*E*)-2-bromobenzaldehyde 4-cyanophenylhydrazone (I) and (*E*)-4-cyanobenzaldehyde 2-bromophenylhydrazone (II) (Fig. 6). We have also examined compounds in which the halogen or nitrile has been replaced by a group of similar size and shape in order to determine both the effect of disrupting any Lewis acid–Lewis base contacts and the possibility of further isostructuralism. We report here two additional isostructural pairs we have identified in this manner: *N*-(2-trifluoromethylbenzylidene)-2-methylaniline (III) and *N*-(2-methylbenzylidene)-2-trifluoromethylaniline (IV); *N*-(2-bromobenzylidene)-2-methylaniline (V) and *N*-(2-methylbenzylidene)-2-bromoaniline (VI). We also describe here the crystal structures of *N*-(4-methylbenzylidene)-4-cyanoaniline (VII) and *N*-(4-cyanobenzylidene)-4-methylaniline (VIII), which although closely similar in unit-cell dimensions proved not to be identical in molecular-packing arrangement and thus qualified in our investigation as a 'near miss'. We did, however, find the packing arrangement of (VIII) to be similar to that of the chloro-methyl benzylideneanilines MBZCLA/MBZCLB.

2. Experimental

Compounds (I)–(VIII) were prepared from the corresponding substituted aldehydes and anilines using a standard method (a mixture composed of approximately 0.5 g of each reactant refluxed in ethanol for usually 15–30 min) and were crystallized from ethanol, unless otherwise noted. Melting points were determined using a Gallenkamp melting point apparatus and are uncorrected. Both (I) and (II) were obtained as yellow needles with broad melting points; the onset of melting occurred for (I) at 473 K with gradual melting/decomposition continuing past 503 K, while the onset of melting occurred for (II) at 431 K and continued past 493 K. Both (III) and (IV)

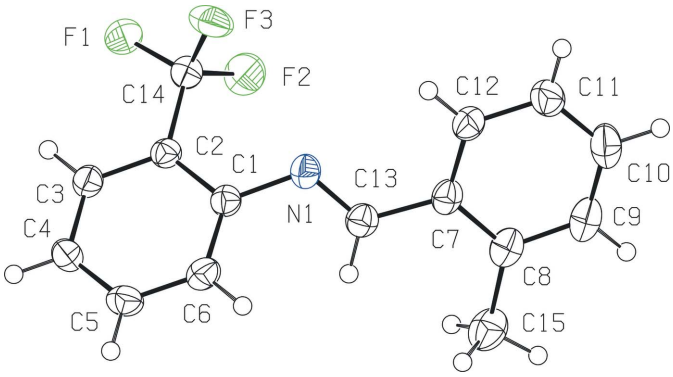

Figure 10
Molecular structure of (IV), showing the atom numbering. Anisotropic displacement ellipsoids are shown at the 50% probability level.

were obtained as greenish-yellow prisms, (III) melting at 326–329 K and (IV) melting at 345–347 K. The isomeric pair (V) and (VI) showed a greater difference in appearance than pairs (I):(II) and (III):(IV), with (V) crystallizing from ethyl acetate as greenish-yellow prisms melting at 351–353 K and (VI) crystallizing from ethanol as orange–yellow prisms melting at 352–355 K. Like (V) and (VI), the pair (VII) and (VIII) differed in color; (VII) was obtained as orange–yellow plates melting at 402–404 K, while (VIII) was obtained as greenish-yellow prisms melting at 417–419 K.

Data sets were collected at 173 K using either a Siemens or Bruker AXS *SMART* system (Bruker, 2001) with Mo $K\alpha$ radiation. Cell refinement and data reduction were accomplished using *SAINT-Plus* (Bruker, 2003). Absorption corrections were applied to all data sets using *SADABS* (Blessing, 1995; Bruker, 2000). The structures were solved and refined using the *SHELXTL* software package (Bruker, 2000); the experimental details are listed in Table 1.[1] In all eight structures, H atoms bonded to C atoms were placed in calculated positions and refined as riding. In (I) and (II), the H atoms bonded to N atoms were located in difference maps and their positions were refined. Graphics were prepared using *PLATON* (Spek, 2003).

3. Results

3.1. Isostructural phenylhydrazones (I) and (II)

Atom-numbering schemes for (I) and (II) are shown in Figs. 7 and 8, respectively. Bond lengths and angles are normal. Both molecules have the *E* configuration with respect to the C=N bond and both molecules are nearly planar, with the rings tilted only a few degrees out of the plane of the three non-hydrogen bridge atoms (Table 2). The bromine-substituted ring of (I) is tilted further out of the plane of these bridge atoms than the bromine-substituted ring of (II), in which a close intramolecular contact occurs between the Br atom and the bridging N—H hydrogen atom [Br···H = 2.72 (3), Br···N 3.095 (2), N—H distance 0.75 (3) Å, N—H···Br = 114 (2)°].

Also shown in Figs. 7 and 8 are close intermolecular interactions involving the nitrile groups of (I) and (II). No close approaches of the Lewis acid–base type between the Br atoms

Table 3
Hydrogen-bond parameters (Å, °).

D—H···*A*	*D*—H	H···*A*	*D*···*A*	*D*—H···*A*
(I)				
N2—H1N···N3	0.78 (3)	2.35 (3)	3.108 (4)	164 (3)
(II)				
N2—H1N···N3	0.75 (3)	2.64 (3)	3.341 (4)	155 (3)
N2—H1N···Br1	0.75 (3)	2.72 (3)	3.095 (2)	113 (2)

Table 4
Angles (°) between least-squares planes in (III)–(VIII).

	A ∠ *B*	*C* ∠ *B*
(III)	5.26 (0.08)	48.84 (0.08)
(IV)	44.85 (0.08)	12.24 (0.12)
(V) (major component)	8.70 (1.60)	40.12 (0.87)
(V) (minor component)	4.98 (2.68)	32.67 (1.89)
(VI)	39.47 (0.15)	6.66 (0.24)
(VII)	6.59 (0.12)	48.73 (0.07)
(VIII)	17.53 (0.22)	10.67 (0.25)

A = plane defined by ring atoms C1–C6; *B* = plane defined by atoms C1, C7, C13 and N1; *C* = plane defined by ring atoms C7–C12.

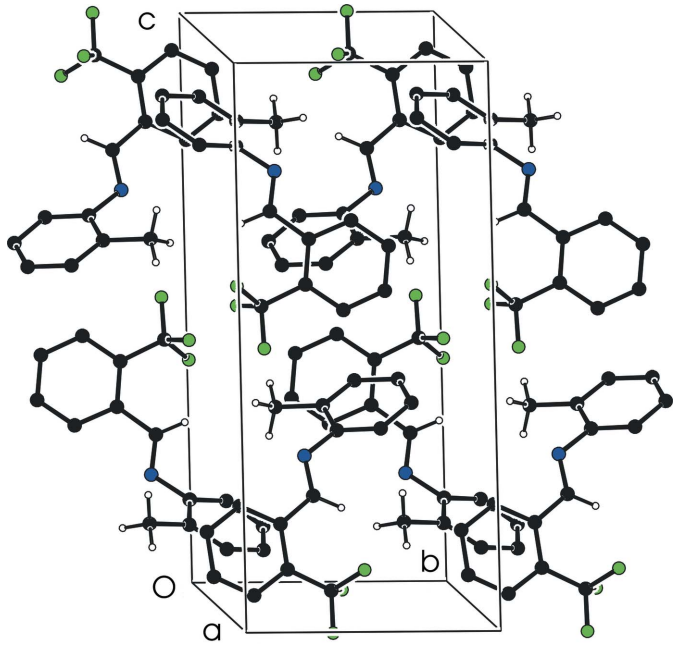

Figure 11
Packing arrangement assumed by both (III) and (IV) [shown here for (III)]. For clarity, the ring H atoms have been omitted.

[1] Supplementary data for this paper are available from the IUCr electronic archives (Reference: GP5015). Services for accessing these data are described at the back of the journal.

and nitrile groups occur; instead, the nitrile group participates in hydrogen bonding. In the previously reported isostructural phenylhydrazone pair LAWJAV and LAWCOC (Ferguson *et al.*, 2005), chains of molecules are formed in which one of the linking interactions is a bifurcated hydrogen bond between an (acceptor) O atom of a nitro group of a given molecule and the two hydrogen-bond donor groups (N—H and C—H) of the bridge of a neighboring molecule, an $R_2^1(6)$ motif. A similar motif occurs in (I) and (II), where the nitrile N atom of a given molecule interacts with both hydrogen-bond donors of the bridge of a neighboring molecule and likewise links the molecules into chains (Table 3); however, these chains are more irregular in shape than those in LAWJAV and LAWCOC. In the LAWJAV and LAWCOC structures, two additional hydrogen bonds, both of the C—H···O type, link each molecule to its neighbor within the chain, with the result that the molecules are effectively pinned into a position in which their long molecular axes are approximately parallel. Molecules within the chain are related by translation. In contrast, (I) and (II) lack additional hydrogen-bonding groups that would serve this function. In (I) and (II), where the only link between molecules within the chain is the $R_2^1(6)$ interaction, the long axes of neighboring molecules are nearly perpendicular to each other rather than parallel to each other as in LAWJAV and LAWCOC, giving the chain an irregular, zigzag appearance. Molecules within the chain are related by the glide operation.

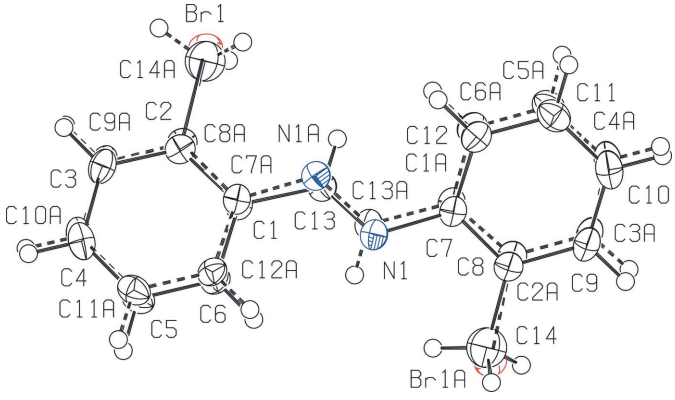

Figure 12
Molecular structure of disordered (V). Atom labels ending in 'A' designate the minor component. The ratio between the two components is 65:35%. For both components, 50% probability ellipsoids are shown.

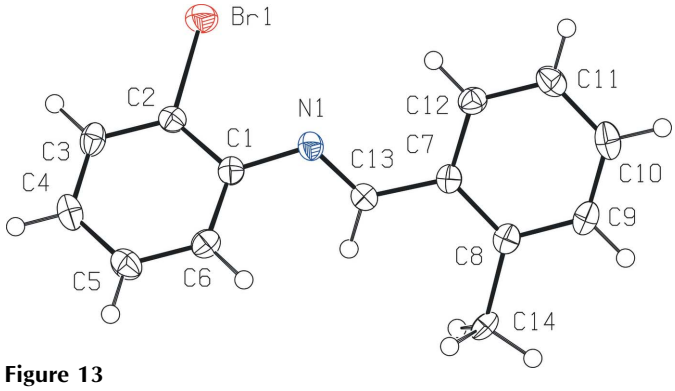

Figure 13
Molecular structure of (VI), showing the atom numbering. Anisotropic displacement ellipsoids are shown at the 50% probability level.

3.2. Isostructural benzylideneanilines (III) and (IV)

Atom-numbering schemes for (III) and (IV) appear in Figs. 9 and 10, respectively. Molecules of both (III) and (IV) are definitely nonplanar (Table 4). In both structures, the aniline ring is tilted farther than the benzylidene ring out of coplanarity with the bridge, in accordance with the conformational tendency ascribed to steric interaction with the bridging H atom noted in §1. The packing arrangement assumed by (III) [and also by (IV)] is shown in Fig. 11. A contact between an F atom of each molecule and a ring H atom of its translationally related neighbor [F3···C4 $(x, -1+y, z)$ approach of 3.2338 (15) Å in (III) and 3.2553 (14) Å in (IV)] links the molecules into chains extending parallel to the **b** axis. There are no close intermolecular contacts, in particular none involving the bridging atoms, that would serve to differentiate the packing arrangements of the two isomers from each other upon reversal of the bridge orientation.

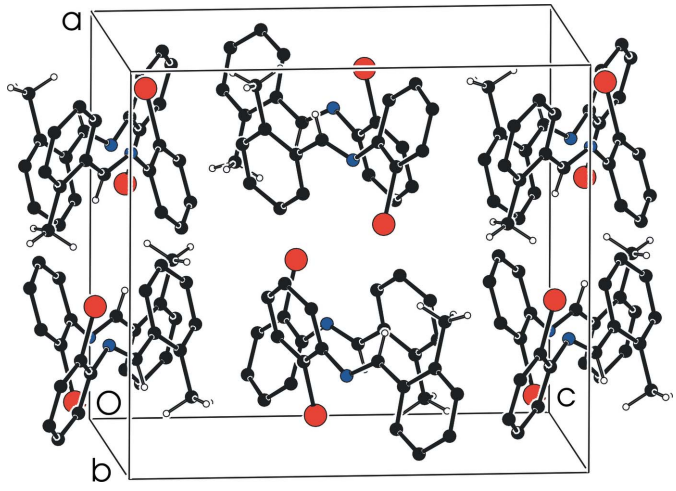

Figure 14
Packing arrangement assumed by both (V) and (VI) [shown here for (VI)]. For clarity, ring H atoms have been omitted.

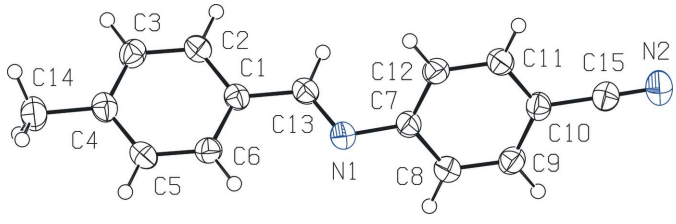

Figure 15
Molecular structure of (VII), showing the atom numbering. Anisotropic displacement ellipsoids are shown at the 50% probability level. One orientation of the disordered methyl group is shown.

3.3. Isostructural benzylideneanilines (V) and (VI)

Views of the molecules (V) and (VI) are shown in Figs. 12 and 13, respectively. Unlike that of the previous isomeric pairs (I):(II) and (III):(IV), the isostructuralism of the pair (V) and (VI) is associated with disorder, particularly in (V). Attempts to refine (V) conventionally failed to yield a final R_1 value less than roughly 0.15. Disorder in benzylideneaniline structures is a common occurrence, often involving four possible orientations of the molecule: two in which the molecule is flipped end-for-end and two in which the molecule is rotated about its long axis (Haller *et al.*, 1995; Harada *et al.*, 2004*a*,*b*). The absence of any significant peaks located just off the midpoint of the bridging C═N bond and the anomalous intensities of the peaks corresponding to the Br atom and the methyl C atom suggested that the disorder could be modeled satisfactorily by an end-for-end flip of the molecule, which would involve the near-superposition of the Br atom and the methyl group in the electron density map. The two orientations of the molecule of (V) in this disorder model are shown in Fig. 12. The two components were refined anisotropically. Distances between ring C atoms and their bromine and methyl substituents were constrained to values of 1.902 and 1.504 Å, respectively, and corresponding angles were also constrained to target values. Anisotropic displacement parameters for those atoms from separate components that were located close to each other in the model were constrained to be equal and the overall geometries of the two components were restrained to be equal. Refinement of this model yielded a final $R_1 = 0.027$ and $wR_2 = 0.063$, the populations of the two orientations refining to 0.6457 (7) and 0.3543 (7). The resulting bridge C═N bond length of 1.271 (5) Å in (V) is consistent with values found in models of other disordered benzylideneanilines (Harada *et al.*, 2004*a*). In contrast, although the presence of small peaks near the methyl C atom and the bridge N atom of (VI) suggested a small percentage of end-for-end disorder similar to that found in (V), refinement of an ordered model for (VI) proved satisfactory. The orientation of (VI) in its unit cell corresponds to that of the minor component of disordered (V). A comparison of the molecular conformations appears in Table

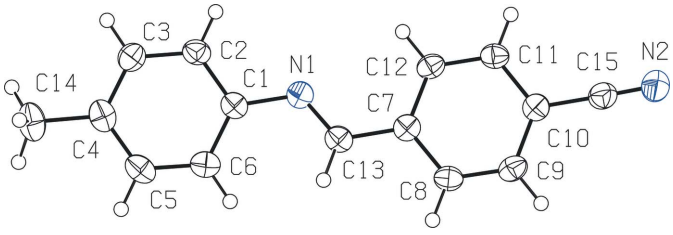

Figure 16
Molecular structure of (VIII), showing the atom numbering. Anisotropic displacement ellipsoids are shown at the 50% probability level.

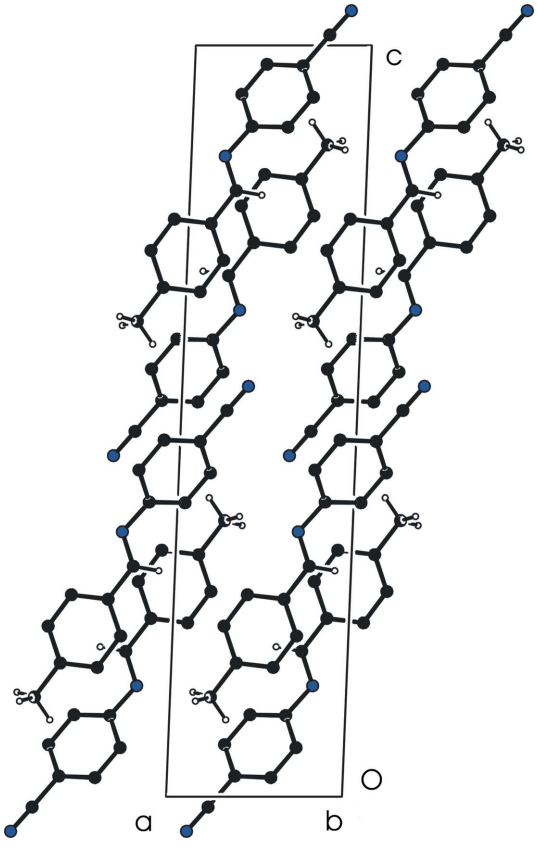

Figure 17
Packing arrangement of (VII) viewed along the *b* axis. For clarity, ring H atoms have been omitted.

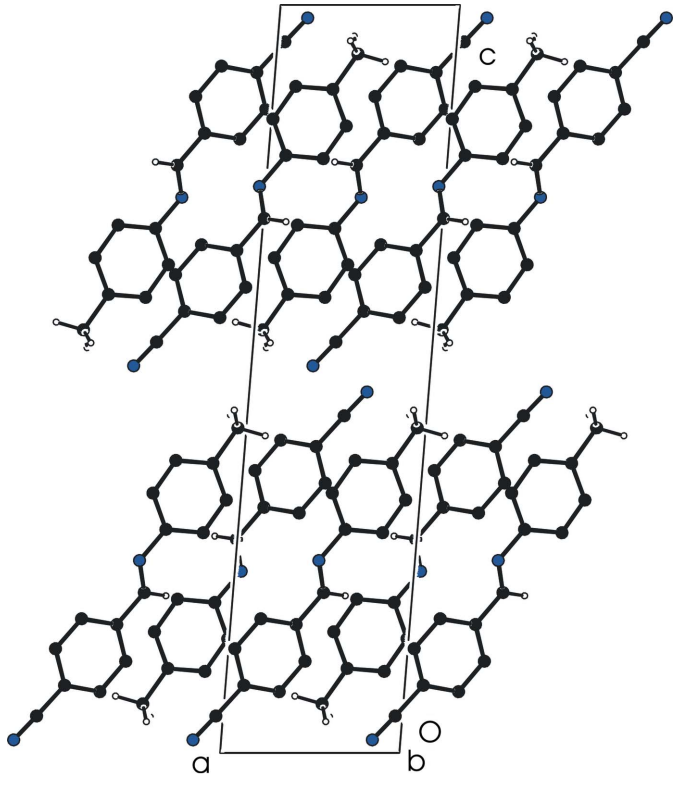

Figure 18
Packing arrangement of (VIII) viewed along the *b* axis. For clarity, ring H atoms have been omitted. Despite the close resemblance between (VII) and (VIII) in cell constants, the packing arrangements are not identical (compare Fig. 17).

4. A view of the packing arrangement assumed by (VI) [and also in disordered fashion by (V)] appears in Fig. 14. Contacts to the Br atoms are all of the Br···H—C type in which the C atom is either a ring carbon or a methyl carbon. There are no close Br···Br or Br···N contacts.

3.4. Benzylideneanilines (VII) and (VIII)

Atom-numbering schemes and molecular conformations for (VII) and (VIII) are shown in Figs. 15 and 16, respectively. Angles between selected molecular planes are given in Table 4. Residual electron density in the difference map of (VII) in the region of the methyl-group H atoms led to the modeling of that group as disordered. The refinement of (VIII) resulted in a rather high value of *R*, perhaps the result of some end-for-end disorder of the molecular position similar to that shown by (V), as suggested in the difference map by a small peak located near the bridge N atom in a location corresponding to the disordered position of the bridge H atom. Attempts to model this disorder were unsuccessful, so given the fact that bond lengths and bond angles (notably the bridge C=N distance and the nitrile C≡N distance) were reasonable, a disordered model was not pursued further. In spite of the general similarity in space-filling requirements between the methyl group and the halogens (especially chlorine and bromine), neither (VII) nor (VIII) is isostructural with the chloro-cyano, bromo-cyano or iodo-cyano 4,4′-disubstituted benzylideneanilines we have examined previously (Ojala *et al.*, 1999; Ojala *et al.*, 2001). Moreover, in spite of their close similarity in cell constants and space-group symmetry, (VII) and (VIII) are not isostructural with each other (Figs. 17 and 18). On the other hand, the packing arrangement of (VIII) resembles that of the chloro-methyl benzylideneanilines MBZCLA/MBZCLB (compare Fig. 18 to Fig. 3 in Haller *et al.*, 1995).

4. Conclusions

We began this work with the assumption that solid-state intermolecular interactions such as classical hydrogen bonding and Lewis acid–Lewis base contacts, interactions of at least moderate strength, might favor isostructuralism between these bridge-flipped isomers by organizing molecules in crystals of different isomers into similar packing motifs. We have found this to be true for (I) and (II), but other examples of isostructuralism we have found, both in the literature and in our own crystallographic studies, occur in cases in which interactions of this type are absent. When they are present, they often prove to play a differentiating role by organizing molecules into *different* packing motifs. For pairs of isomers in which these intermolecular interactions involve the bridging atoms, switching the bridging-atom positions renders isostructuralism unlikely. Such interactions operating intramolecularly (such as intramolecular hydrogen bonding in salicylideneanilines and their bridge-flipped isomers) discourage isostructuralism by enforcing differences in molecular conformation. Although predicting which pairs of isomers will not assume the same packing arrangement thus has a reasonable structural basis, our study so far, although successful in increasing the number of known examples of isostructural bridge-flipped isomers, has not yet given us the ability to predict which pairs of isomers will assume the same packing arrangement or even to suggest substituents or substitution patterns that will facilitate this occurrence. Given the variety of factors that can prevent bridge-flipped isomers from forming isostructural crystals, perhaps our most surprising result thus far is that even this many of them do.

Acknowledgment is made to the Donors of the American Chemical Society Petroleum Research Fund for support of this research. The authors express their thanks to Dr Victor G. Young Jr (Director) and Benjamin E. Kucera of the X-ray Crystallographic Laboratory of the Department of Chemistry, University of Minnesota, Minneapolis, MN, and to Professor Carl Henrik Görbitz of the University of Oslo, Norway, for their assistance. We are grateful to Dr William B. Gleason of the Department of Laboratory Medicine and Pathology of the University of Minnesota, Minneapolis, MN, Dr Doyle Britton of the Department of Chemistry of the University of Minnesota, Minneapolis, MN, Dr Ilia A. Guzei of the Department of Chemistry of the University of Wisconsin, Madison, WI, and Dr Kenneth Haller of the School of Chemistry, Suranaree University of Technology, Nakhon Ratchasima, Thailand, for helpful discussions.

References

Adamson, A. J., Archambeau, Y., Banks, R. E., Beagley, B., Helliwell, M., Pritchard, R. G. & Tipping, A. E. (1994). *Acta Cryst.* C**50**, 967–971.
Allaway, C. L., Daly, M., Nieuwenhuyzen, M. & Saunders, G. C. (2002). *J. Fluorine Chem.* **115**, 91–99.
Allen, F. H. (2002). *Acta Cryst.* B**58**, 380–388.
Bar, I. & Bernstein, J. (1983). *Acta Cryst.* B**39**, 266–272.
Bar, I. & Bernstein, J. (1987). *Tetrahedron*, **43**, 1299–1305.
Bernstein, J. & Bar, I. (1980). *Eur. Cryst. Meet.* **6**, 21.
Blessing, R. H. (1995). *Acta Cryst.* A**51**, 33–38.
Bouwstra, J. A., Schouten, A., Kroon, J. & Helmholdt, R. B. (1985). *Acta Cryst.* C**41**, 420–426.
Bryan, R. F., Forcier, P. & Miller, R. W. (1978). *J. Chem. Soc. Perkin Trans. 2*, pp. 368–372.
Bruker (2000). *SADABS*, Version 2.03, and *SHELXTL*, Version 6.12. Bruker Analytical X-ray Instruments, Madison, Wisconsin, USA.
Bruker (2001). *SMART*, Version 5.054. Bruker Analytical X-ray Instruments, Madison, Wisconsin, USA.
Bruker (2003). *SAINT-Plus*, Version 6.45. Bruker Analytical X-ray Instruments, Madison, Wisconsin, USA.
Bürgi, H. B. & Dunitz, J. D. (1970). *Helv. Chim. Acta*, **53**, 1747–1764.
Bürgi, H. B., Dunitz, J. D. & Züst, C. (1968). *Acta Cryst.* B**24**, 463–464.
Chakraborty, S., Laye, R. H., Paul, R. L., Gonnade, R. G., Puranik, V. G., Ward, M. D. & Lahiri, G. K. (2002). *J. Chem. Soc. Dalton Trans.* pp. 1172–1179.
Clegg, W., Elsegood, M. R. J., Heath, S. L., Houlton, A. & Shipman, M. A. (1996). *Acta Cryst.* C**52**, 2548–2552.
Cole, J. M., Howard, J. A. K. & McIntyre, G. J. (2001). *Acta Cryst.* B**57**, 410–414.
Ferguson, G., Glidewell, C., Low, J. N., Skakle, J. M. S. & Wardell, J. L. (2005). *Acta Cryst.* C**61**, o613–o616.

Filipenko, O. S., Ponomarev, V. I. & Atovmyan, L. O. (1976). *Dokl. Akad. Nauk SSSR*, **229**, 1113–1116.
Filipenko, O. S., Shigorin, V. D., Ponomarev, V. I., Atovmyan, L. O., Safina, Z. Sh. & Tarnopol'skii, B. L. (1977). *Kristallografiya*, **22**, 534–541.
Flack, H. D. (1983). *Acta Cryst.* A**39**, 876–881.
Glidewell, C., Howie, R. A., Low, J. N., Skakle, J. M. S., Wardell, S. M. S. V. & Wardell, J. L. (2002). *Acta Cryst.* B**58**, 864–876.
Haller, K. J., Rae, A. D., Heerdegen, A. P., Hockless, D. C. R. & Welberry, T. R. (1995). *Acta Cryst.* B**51**, 187–197.
Harada, J., Harakawa, M. & Ogawa, K. (2004*a*). *Acta Cryst.* B**60**, 578–588.
Harada, J., Harakawa, M. & Ogawa, K. (2004*b*). *Acta Cryst.* B**60**, 589–597.
He, X., Stowell, J. G., Morris, K. R., Pfeiffer, R. R., Li, H., Stahly, G. P. & Byrn, S. R. (2001). *Cryst. Growth Des.* **1**, 305–312.
Hoshino, N., Inabe, T., Mitani, T. & Maruyama, Y. (1988). *Bull. Chem. Soc. Jpn*, **61**, 4207–4214.
Hursthouse, M. B. & Karaulov, A. (2003). Private communication.
Inabe, T., Hoshino, N., Mitani, T. & Maruyama, Y. (1989). *Bull. Chem. Soc. Jpn*, **62**, 2245–2251.
Jiao, Y.-H., Zhang, Q. & Ng, S. W. (2006). *Acta Cryst.* E**62**, o3614–o3615.
Kamwaya, M. E. & Khoo, L. E. (1985). *J. Fiz. Malays.* **6**, 135–140.
Karakas, A., Elmali, A., Unver, H. & Svoboda, I. (2004). *J. Mol. Struct.* **702**, 103–110.
Li, A., Bin, X., Zhu, S.-Z., Huang, Q.-C. & Liu, J.-S. (1994). *J. Fluorine Chem.* **68**, 145–148.
Lindeman, S. V., Andrianov, V. G., Kravcheni, S. G., Potapov, V. M., Potekhin, K. A. & Struchkov, Y. T. (1981). *Zh. Strukt. Khim.* **22**, 123–131.
Lindeman, S. V., Shklover, V. E. & Struchkov, Y. T. (1981). *Acta Cryst.* A**37**, C87.
Lindeman, S. V., Shklover, V. E., Struchkov, Y. T., Kravcheni, S. G. & Potapov, V. M. (1982*a*). *Cryst. Struct. Commun.* **11**, 43–47.
Lindeman, S. V., Shklover, V. E., Struchkov, Y. T., Kravcheni, S. G. & Potapov, V. M. (1982*b*). *Cryst. Struct. Commun.* **11**, 49–52.
Meunier-Piret, J., Germain, G., Declercq, J. P. & van Meerssche, M. (1982*a*). *Bull Soc. Chim. Belg.* **91**, 89–90.
Meunier-Piret, J., Germain, G., Declercq, J. P. & van Meerssche, M. (1982*b*). *Bull. Soc. Chim. Belg.* **91**, 93–94.
Meunier-Piret, J., Piret, P., Germain, G. & van Meerssche, M. (1972). *Bull. Soc. Chim. Belg.* **81**, 533–538.
Morimoto, M., Kobatake, S. & Irie, M. (2003). *J. Am. Chem. Soc.* **125**, 11080–11087.
Moustakali-Mavridis, I., Hadjoudis, E. & Mavridis, A. (1978). *Acta Cryst.* B**34**, 3709–3715.
Nakai, H., Ezumi, K. & Shiro, M. (1981). *Acta Cryst.* B**37**, 193–197.
Nakai, H., Shiro, M., Ezumi, K., Sakata, S. & Kubota, T. (1976). *Acta Cryst.* B**32**, 1827–1833.
Navon, O. & Bernstein, J. (1997). *Struct. Chem.* **8**, 3–11.
Ojala, C. R., Ojala, W. H., Gleason, W. B. & Britton, D. (1999). *J. Chem. Cryst.* **29**, 27–32.
Ojala, C. R., Ojala, W. H., Gleason, W. B. & Britton, D. (2001). *J. Chem. Cryst.* **31**, 377–386.
Orr, L. B., Jr, Parsons, E. J. & Pennington, W. T. (1992). *Acta Cryst.* C**48**, 2042–2043.
Patani, G. A. & LaVoie, E. J. (1996). *Chem. Rev.* **96**, 3147–3176.
Ponomarev, V. I., Filipenko, O. S., Atovmyan, L. O., Grazhulene, S. S., Lempert, S. A. & Shigorin, V. D. (1977). *Kristallografiya (Russ.) (Crystallogr. Rep.)* **22**, 394–396.
Shan, S., Wang, X.-J., Hu, W.-X. & Xu, D.-J. (2004). *Acta Cryst.* E**60**, o1954–o1956.
Sheldrick, G. M. (1990). *Acta Cryst.* A**46**, 467–473.
Sheldrick, G. M. (1997). *SHELXL*97 and *SHELXS*97. University of Göttingen, Germany.
Silverman, R. B. (2004). *The Organic Chemistry of Drug Design and Drug Action*, 2nd ed. pp. 29–34. New York: Elsevier, Inc.
Spek, A. L. (2003). *J. Appl. Cryst.* **36**, 7–13.
Tanaka, M., Imai, T., Goto, T., Taka, J.-I., Akamatsu, M., Kashino, S. & Mogi, K. (1998). *Bull. Chem. Soc. Jpn*, **71**, 2561–2571.
Tunc, T., Tezcan, H., Sari, M., Buyukgungor, O. & Yagbasan, R. (2003). *Acta Cryst.* C**59**, o528–o529.
Velavan, R., Sivakumar, K. & Anbu, M. (1995). *Acta Cryst.* C**51**, 1227–1229.
Vickery, B., Willey, G. R. & Drew, M. G. B. (1985). *Acta Cryst.* C**41**, 1072–1075.
Wardell, J. L., Skakle, J. M. S., Low, J. N. & Glidewell, C. (2005). *Acta Cryst.* C**61**, o10–o14.
Wardell, J. L., Wardell, S. M. S. V., Skakle, J. M. S., Low, J. N. & Glidewell, C. (2002). *Acta Cryst.* C**58**, o428–o430.
Welberry, T. R., Butler, B. D. & Heerdegen, A. P. (1993). *Acta Chim. Hung.* **130**, 327–345.
Whitney, J. F. & Corvin, I. (1949). *Anal. Chem.* **21**, 306–307.
Yeap, G.-Y., Fun, H.-K., Teoh, S.-G., Teo, S.-B., Chinnakali, K. & Yip, B.-C. (1992). *Acta Cryst.* C**48**, 2257–2258.
Yin, Z.-G., Qian, H.-Y., Jia, J., Zhou, N. & Feng, L.-Q. *Acta Cryst.* E**62**, o4913–o4914.
Zamir, S. & Bernstein, J. (1993). *Acta Chim. Hung.* **130**, 301–325.